

Supplementary Materials

**A skin-wearable and self-powered laminated pressure sensor based on triboelectric nanogenerator for monitoring human motion**

**Agha Aamir Jan<sup>#</sup>, Seungbeom Kim<sup>#</sup>, Seok Kim<sup>\*</sup>**

Department of Mechanical Engineering, Pohang University of Science and Technology (POSTECH), Pohang 37673, Republic of Korea.

<sup>#</sup>Authors contributed equally.

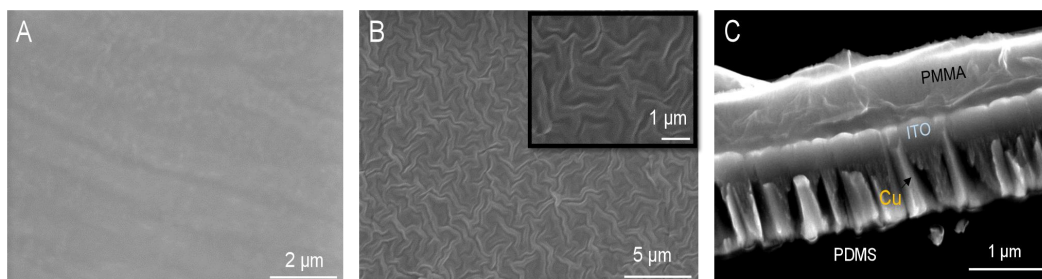
**\*Correspondence to:** Prof. Seok Kim, Department of Mechanical Engineering, Pohang University of Science and Technology (POSTECH), 77 Cheongam-Ro, Pohang 37673, Republic of Korea. E-mail: [seok.kim@postech.ac.kr](mailto:seok.kim@postech.ac.kr)



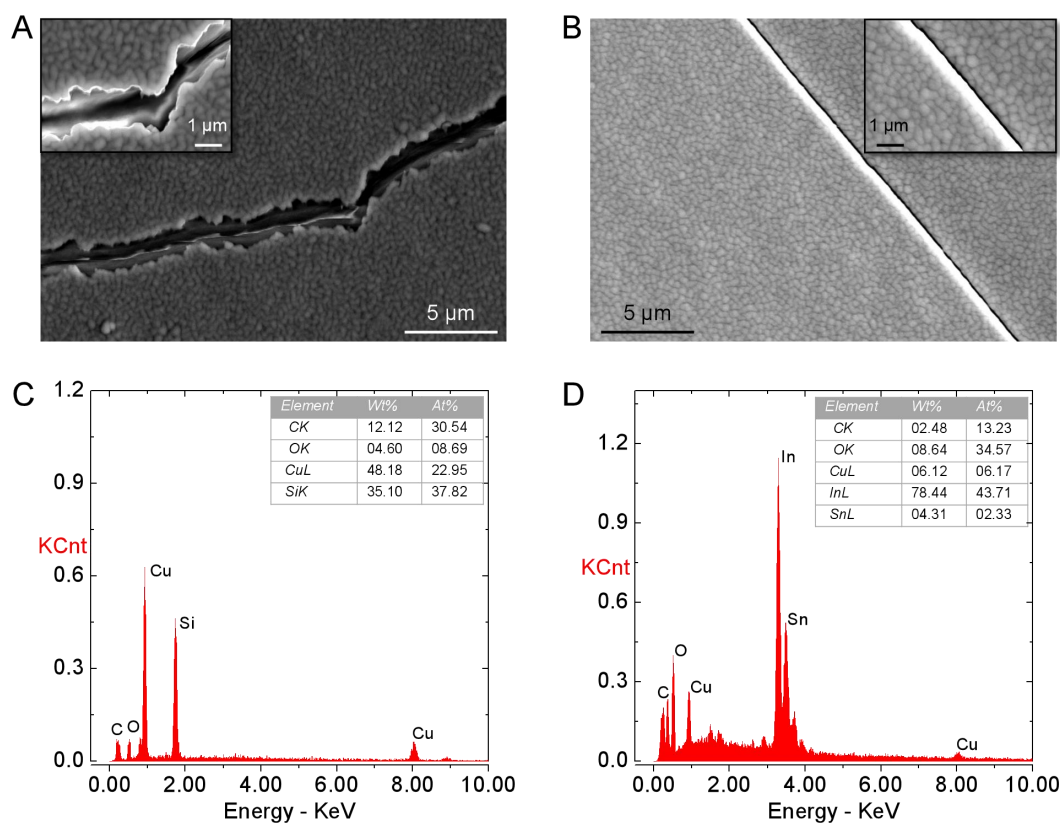
© The Author(s) 2021. Open Access This article is licensed under a Creative Commons Attribution 4.0 International License (<https://creativecommons.org/licenses/by/4.0/>), which permits unrestricted use, sharing, adaptation, distribution and reproduction in any medium or

format, for any purpose, even commercially, as long as you give appropriate credit to the original author(s) and the source, provide a link to the Creative Commons license, and indicate if changes were made.



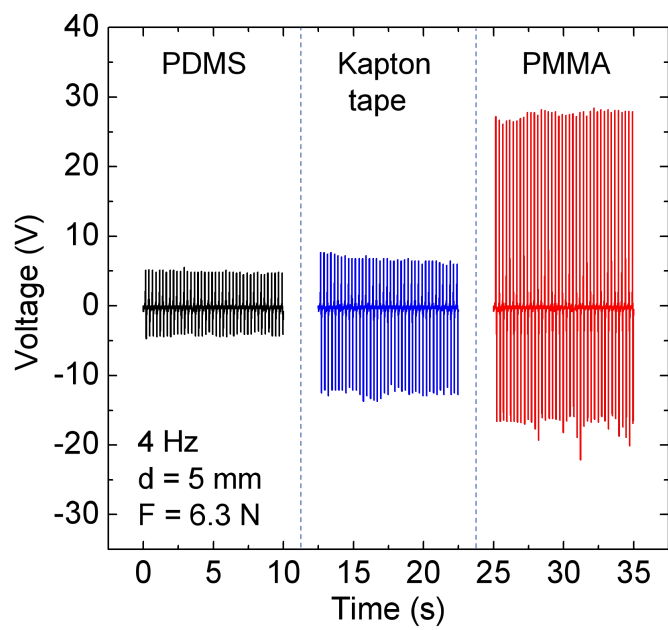


**Supplementary Figure 1.** Scanning electron microscopy (SEM) images. (A) Pristine PDMS after peeling off from mold; (B) O<sub>2</sub> plasma treated (O-PDMS), and the magnified view of O-PDMS top surface; (C) The cross-sectional view of tribo-positive layer PMMA coated on ITO/Cu electrode.

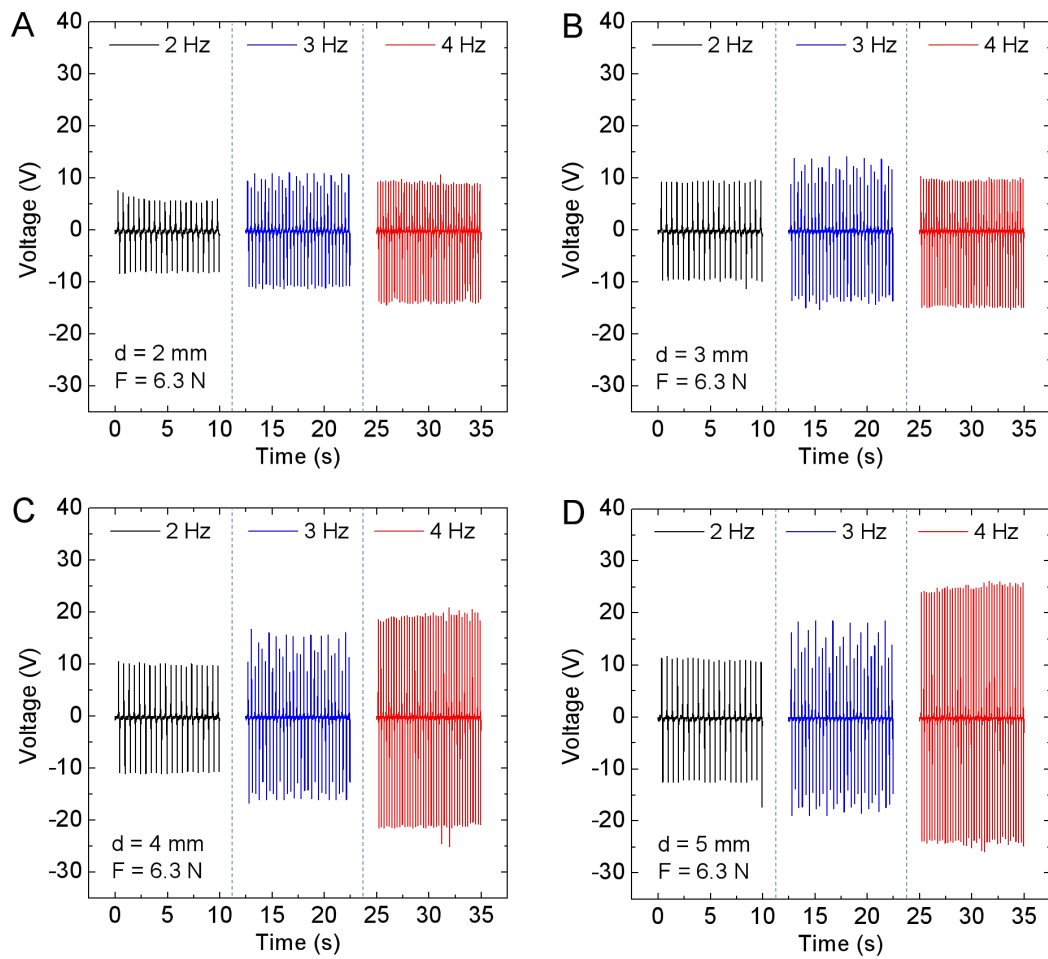


**Supplementary Figure 2.** SEM and energy dispersive x-ray (EDX) analysis of cracked Cu and ITO-filled crack in Cu deposited on O-PDMS. (A) SEM image of a crack on Cu electrode deposited on O-PDMS with magnified image of crack (inset); (B) ITO-filled crack on Cu/O-PDMS; (C) EDX spectra of crack on the Cu/O-PDMS; and (D) EDX spectra of ITO-filled crack of Cu/O-PDMS.

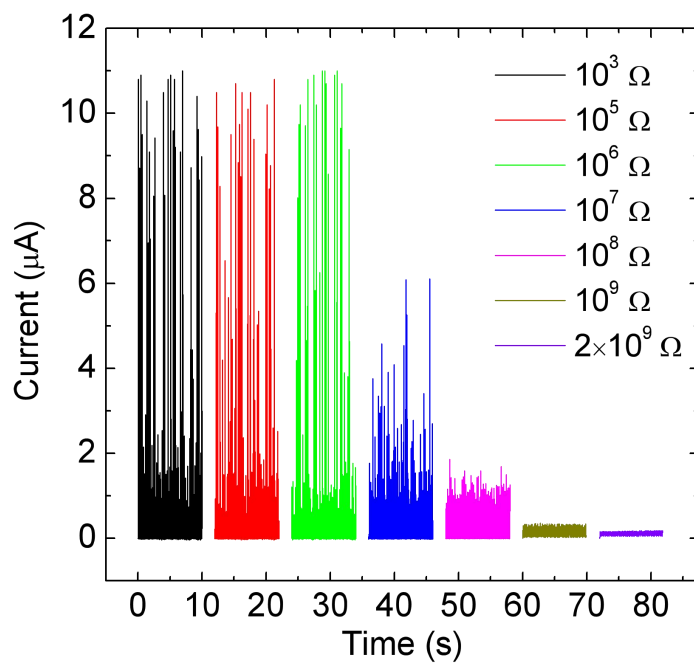
The SEM image [Supplementary Figure 2B] clearly displays the ITO-filled crack. The EDX spectra of cracked copper [Supplementary Figure 2C] indicate the presence of silicon (Si) originating from the PDMS substrate. This suggests that there was no electrical path through the crack. Conversely, in the EDX spectra of the crack filled with ITO [Supplementary Figure 2D], the highest atomic percent was attributed to indium. Additionally, the electrical conductivity measurements for the copper electrode and ITO/Cu electrode yielded values of 8.7 and 75.8 S/m, respectively. These findings imply that the inclusion of an ITO layer within the cracks on the copper electrode establishes a conductive layer, thereby enhancing the overall conductivity and performance of the electrode.



**Supplementary Figure 3.** The output voltage of PTFE film under triboelectric contact with PDMS, Kapton tape, and PMMA on ITO/Cu electrode.

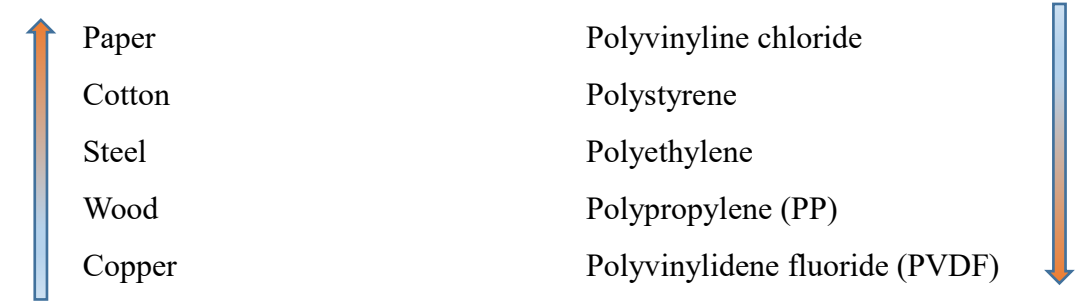


**Supplementary Figure 4.** The cyclic output voltage output as a function of tapping frequency (2, 3, and 4 Hz) at tapping force 6.3 N, and different separation gaps (A) Separation gap,  $d = 2$  mm; (B)  $d = 3$  mm; (C)  $d = 4$  mm; (D)  $d = 4$  mm.



**Supplementary Figure 5.** The rectified current output at various ohmic loads from  $10^3$  to  $2 \times 10^9 \Omega$ .

**Supplementary Table 1.** Triboelectric series of some commonly used materials according to the tendency of accepting electrons (tribo-negative) to donating electrons (tribo-positive). When two materials are far apart on the triboelectric series, more effective charge transfer takes place.

	Glass	Polychlorobutadiene	
	Wool	Natural rubber	
	Polyamide 6-6 (Nylon)	Polyacrilonitrile	
	Silk	Polybisphenol carbonate	
	Aluminium	Polychloroether	
	Paper	Polyvinyl chloride	
	Cotton	Polystyrene	
	Steel	Polyethylene	
	Wood	Polypropylene (PP)	
	Copper	Polyvinylidene fluoride (PVDF)	
	Silver	Polyimide (Kapton)	
	<b>Polymethyl methacrylate (PMMA)</b>	Polyvinyl chloride (PVC)	
	Polyvinyl alcohol (PVA)	Polydimethylsiloxane (PDMS)	
	Polyester	<b>Polytetrafluoroethylene (PTFE)</b>	

**Supplementary Table 2. Comparison of wide-range pressure sensitivity of LF-TENG with other TENG based pressure sensors**

<b>Authors</b>	<b>Active Materials</b>	<b>Sensitivity Range-I (0.0245-1.23 kPa)</b>	<b>Sensitivity Range-II (2.45-23.3 kPa)</b>
Liu <i>et al.</i> <sup>[1]</sup>	PDMS microsphere-FEP	150 V/kPa, 26.6 V/kPa (0.005-0.18 kPa) (0.18-1 kPa)	Not reported
Zheng <i>et al.</i> <sup>[2]</sup>	Chitosan-FEP film	Not reported	46.03 V/kPa (1.25-6.25 kPa)
Zhong <i>et al.</i> <sup>[3]</sup>	Wire mesh-structured PDMS	44.31 V/kPa (0.006-2 kPa)	7.16 V/kPa (2-8.5 kPa)
Zhu <i>et al.</i> <sup>[4]</sup>	Fluorinated ethylene propylene (FEP)-PET/ITO	44 V/kPa (0.03-0.15 kPa)	0.5 V/kPa (2-10 kPa)
Garcia <i>et al.</i> <sup>[5]</sup>	PVDF/ PVP electrospun fibers	8.8 V/kPa, 3.9 V/kPa (0.2-0.8 kPa) (0.8-1.6 kPa)	Not reported
This work	PDMS encapsulated PTFE-PMMA thin film	7.287 V/kPa (0.0245-1.23 kPa)	0.663 V/kPa (2.45-23.3 kPa)
Rao <i>et al.</i> <sup>[6]</sup>	PDMS-BiTO/rGO/PVDF	5.07 V/kPa (0.2-1.72 kPa)	1.89 V/kPa (1.72-3.65 kPa)
He <i>et al.</i> <sup>[7]</sup>	PDMS-PI-Cu	Not reported	0.367 V/kPa (3-45 kPa)
Rasel <i>et al.</i> <sup>[8]</sup>	PDMS- PDMS/CNT Micro structured by sandpaper	Not reported	0.35 V/kPa (5- 50 kPa)
Cao <i>et al.</i> <sup>[9]</sup>	Mxene on prestretched latex substrate	2.35 V/kPa (0.3-1 kPa)	0.14 V/kPa (1-50 kPa)
Lou <i>et al.</i> <sup>[10]</sup>	PVDF/AgNW- conductive PU fabric	1.67 V/kPa (0-3 kPa)	0.20 V/kPa (3-32 kPa)
Lin <i>et al.</i> <sup>[11]</sup>	PDMS ion hydrogel-PVDF-HFP	0.43 V/kPa (0.01-1.5 kPa)	0.068 V/kPa (100-700 kPa)



core-shell fiber mats			
Zhao <i>et al.</i> <sup>[12]</sup>	Cu-coated polyacrylonitrile (Cu-PAN) yarns and parylene coated Cu-PAN	0.344 V/kPa (0-0.25 kPa)	0.018 V/kPa (0.25-37.5 kPa)
Wang <i>et al.</i> <sup>[13]</sup>	PDMS-Al	Not reported	0.06 V/kPa (1-80 kPa)
Pu <i>et al.</i> <sup>[14]</sup>	PAAm-LiCl hydrogel/PDMS	Not reported	0.013 V/kPa (1.3-70 kPa)

## REFERENCES

1. Liu Z, Zhao Z, Zeng X, Fu X, Hu Y. Expandable microsphere-based triboelectric nanogenerators as ultrasensitive pressure sensors for respiratory and pulse monitoring. *Nano Energy*. 2019;59:295-301. DOI:10.1016/j.nanoen.2019.02.057
2. Zheng Z, Yu D, Wang B, Guo Y. Ultrahigh sensitive, eco-friendly, transparent triboelectric nanogenerator for monitoring human motion and vehicle movement. *Chemical Engineering Journal*. 2022;446:137393. DOI:10.1016/j.cej.2022.137393
3. Zhong Y, Wang J, Han L, et al. High-performance flexible self-powered triboelectric pressure sensor based on chemically modified micropatterned PDMS film. *Sens Actuators A Phys*. 2023;349:114013. DOI:10.1016/j.sna.2022.114013
4. Zhu G, Yang WQ, Zhang T, et al. Self-powered, ultrasensitive, flexible tactile sensors based on contact electrification. *Nano Lett*. 2014;14(6):3208-3213. DOI:10.1021/nl5005652
5. Garcia C, Trendafilova I, Guzman de Villoria R, Sanchez del Rio J. Self-powered pressure sensor based on the triboelectric effect and its analysis using dynamic mechanical analysis. *Nano Energy*. 2018;50:401-409. DOI:10.1016/j.nanoen.2018.05.046
6. Rao J, Chen Z, Zhao D, et al. Tactile electronic skin to simultaneously detect and distinguish between temperature and pressure based on a triboelectric nanogenerator. *Nano Energy*. 2020;75:105073. DOI:10.1016/j.nanoen.2020.105073
7. He J, Xie Z, Yao K, et al. Trampoline inspired stretchable triboelectric nanogenerators as tactile sensors for epidermal electronics. *Nano Energy*. 2021;81:105590. DOI:10.1016/j.nanoen.2020.105590
8. Rasel MS, Maharjan P, Salauddin Md, et al. An impedance tunable and highly efficient triboelectric nanogenerator for large-scale, ultra-sensitive pressure sensing applications. *Nano Energy*. 2018;49:603-613. DOI:10.1016/j.nanoen.2018.04.060
9. Cao Y, Guo Y, Chen Z, et al. Highly sensitive self-powered pressure and strain sensor based on crumpled MXene film for wireless human motion detection. *Nano Energy*. 2022;92:106689. DOI:10.1016/j.nanoen.2021.106689
10. Lou M, Abdalla I, Zhu M, Yu J, Li Z, Ding B. Hierarchically Rough Structured and Self-Powered Pressure Sensor Textile for Motion Sensing and Pulse Monitoring. *ACS Appl Mater Interfaces*. 2020;12(1):1597-1605. DOI:10.1021/acsami.9b19238
11. Lin MF, Xiong J, Wang J, Parida K, Lee PS. Core-shell nanofiber mats for tactile

pressure sensor and nanogenerator applications. *Nano Energy*. 2018;44:248-255.

DOI:10.1016/j.nanoen.2017.12.004

12. Zhao Z, Huang Q, Yan C, et al. Machine-washable and breathable pressure sensors based on triboelectric nanogenerators enabled by textile technologies. *Nano Energy*.

2020;70:104528. DOI:10.1016/j.nanoen.2020.104528

13. Wang X, Zhang H, Dong L, et al. Self-powered high-resolution and pressure-sensitive triboelectric sensor matrix for real-time tactile mapping. *Advanced*

*Materials*. 2016;28(15):2896-2903. DOI:10.1002/adma.201503407

14. Pu X, Liu M, Chen X, et al. Ultrastretchable, transparent triboelectric nanogenerator as electronic skin for biomechanical energy harvesting and tactile

sensing. *Sci Adv*. 2017;3(5):e1700015. DOI:10.1126/sciadv.1700015